

3D Euler about a 2D Symmetry Plane

Miguel D. Bustamante^{1,*} and Robert M. Kerr¹

¹*Mathematics Institute, University of Warwick, Coventry CV4 7AL, United Kingdom*

Initial results from new calculations of interacting anti-parallel Euler vortices are presented with the objective of understanding the origins of singular scaling presented by Kerr (1993) and the lack thereof by Hou and Li (2006). Core profiles designed to reproduce the two results are presented, new more robust analysis is proposed, and new criteria for when calculations should be terminated are introduced and compared with classical resolution studies and spectral convergence tests. Most of the analysis is on a $512 \times 128 \times 2048$ mesh, with new analysis on a just completed $1024 \times 256 \times 2048$ used to confirm trends. One might hypothesize that there is a finite-time singularity with enstrophy growth like $\Omega \sim (T_c - t)^{-\gamma_\Omega}$ and vorticity growth like $\|\omega\|_\infty \sim (T_c - t)^{-\gamma}$. The new analysis would then support $\gamma_\Omega \approx 1/2$ and $\gamma > 1$. These represent modifications of the conclusions of Kerr (1993). Issues that might arise at higher resolution are discussed.

PACS numbers: 47.10.A-, 47.11.Kb, 47.15.ki

Keywords: Euler equations, fluid singularities, vortex dynamics.

I. INTRODUCTION

One definition of solving Euler's three-dimension incompressible equations [1] is determining whether or not they dynamically generate a finite-time singularity if the initial conditions are smooth, in a bounded domain and have finite energy. The primary analytic constraint that must be satisfied [2] is:

$$\int_0^T \|\omega\|_\infty dt \rightarrow \infty \quad (1)$$

where $\|\omega\|_\infty$ is the maximum of vorticity over all space. To date, Kerr (1993) [3] remains the only fully three-dimensional simulation of Euler's equations with evidence for a singularity consistent with this and related constraints [4]. Growth of the enstrophy production and stretching along the vorticity, plus collapse of positions, supported this claim [3]. Additional weaker evidence related to blow-up in velocity and collapsing scaling functions was presented later [5].

There is only weak numerical evidence supporting these claims [6, 7]. In a recent paper, as described in one of the invited talks of this symposium, Hou and Li (2006) [8] found evidence that the above scenario failed at late times.

This contribution will first comment on four issues raised at the symposium, then present preliminary new results. The four issues are:

- How should spurious high-wavenumber energy in spectral methods be suppressed?
- What criteria should be used to determine when numerical errors are substantial?
- What effect do the initial conditions have on singular trends? A cleaner initial condition is proposed.

- We introduce a new approach for determining whether there is singular behavior of the primary properties and the associated scaling. This is applied to both new and old data.

All calculations will be in the following domain: $L_x \times L_y \times L_z = 4\pi \times 4\pi \times 2\pi$ with free-slip symmetries in y and z and periodic in x with up to $n_x \times n_y \times n_z = 1024 \times 256 \times 2048$ mesh points. Using these symmetries only one-half of one of the anti-parallel vortices needs to be simulated.

The “symmetry” plane will be defined as xz free-slip symmetry through the maximum perturbation of the initial vortices and the “dividing” plane will be defined as the xy free-slip symmetry between the vortices.

II. HOW SHOULD SPURIOUS HIGH-WAVENUMBER ENERGY IN SPECTRAL METHODS BE SUPPRESSED?

A generic difficulty in applying spectral methods to localized physical space phenomena is the accumulation of spurious high-wavenumber energy that leads to numerical errors.

What is the best approach for eliminating these spurious modes? We have compared the old-fashioned 2/3rds dealiasing versus the recently proposed 36th-power hyperviscous filter [8, 11]. Detailed tests to be described in a later paper show that the latter is better in the sense that for several quantities, such as the peak vorticity, lower resolution calculations follow the high resolution cases longer. But a combination of the two approaches works even better, and that is what is used here.

Still, caution is required for any of these approaches as the hyperviscosity can dissipate small structures such as the anomalous negative vorticity in the squared-off profile below. Surprisingly the 36th-order hyperviscosity does not appear to produce the ghost vortices that are a known artifact of lower-order schemes.

*Electronic address: mig'busta@yahoo.com

III. WHAT CRITERIA SHOULD BE USED TO DETERMINE WHEN NUMERICAL ERRORS ARE SUBSTANTIAL?

There are traditionally two approaches to this problem, one emphasizing local quantities such as $\|\boldsymbol{\omega}\|_\infty$, and the other emphasizing global quantities such as the mean square vorticity or enstrophy. We use both.

1. Local quantities and resolution

To determine local resolution it is important to check the convergence of local quantities such as:

- The maximum of vorticity $\|\boldsymbol{\omega}\|_\infty$. The location of $\|\boldsymbol{\omega}\|_\infty$ will be defined as \boldsymbol{x}_∞ .
- The local stretching of vorticity

$$\alpha = \hat{\omega}_i e_{ij} \hat{\omega}_j \quad (2)$$

where $\hat{\omega} = \boldsymbol{\omega}/|\boldsymbol{\omega}|$ and $e_{ij} = \frac{1}{2}(u_{i,j} + u_{j,i})$.

Following earlier work [3, 8], we use the criteria that \boldsymbol{x}_∞ cannot be closer than 6 mesh points from the dividing plane.

2. Integral quantities

Examples of integral quantities we could monitor are: energy, circulation (which are in principle conserved), enstrophy and helicity (which are in principle changing).

- Energy is robustly conserved by spectral methods even when under-resolved and therefore is not a useful test. Convergence of the energy spectrum [8] is only a partial test because it neglects phase errors.
- Circulation in the upper half of the symmetry plane (i.e., the $z > 0$ half of the xz -plane, which is perpendicular to the primary direction of vorticity y) is conserved. Circulation in the equivalent half of the dividing plane is also conserved. In all of the initial conditions considered here, it is initially zero and ideally should remain so. Therefore, the circulations of the symmetry and dividing planes, $\sigma_y = \int_{z>0} \omega_y(x, 0, z, t) dx dz$ and $\sigma_z = \int_{y>0} \omega_z(x, y, 0, t) dx dy$ were monitored.

We have found that serious depletion of σ_y is controlled by n_z and the time this begins is independent of the high-wavenumber filter. Once n_z is set, by convergence of $\|\boldsymbol{\omega}\|_\infty$, we find that there is good convergence if $n_x = n_z/2$ and $n_y = n_z/4$. A later paper will provide more details on these convergence tests. We will violate the condition on n_y at late times due to current memory restrictions.

Without the circulation test, it is difficult to draw conclusions about the late times in Hou and Li (2006) [8] where they claim to see divergence from the scaling of Kerr (1993) [3].

- Enstrophy Ω grows in time, so one test is to check how it is balanced by its production Ω_p , which we determine directly. The enstrophy and its production are

$$\Omega = \int dV \omega^2, \quad \Omega_p = 2 \int dV \omega_i e_{ij} \omega_j. \quad (3)$$

- Helicity grows within the quadrant simulated (not over the full anti-parallel geometry), but its production is determined by pressure which has not been calculated.

IV. WHAT IS THE EFFECT OF THE INITIAL CONDITIONS ON THE POTENTIALLY SINGULAR BEHAVIOR?

A. Earlier descriptions

Because ambiguities in the earlier description of the initial condition of [3] led to differences in the initial condition of Hou and Li (2006) [8], the community needs a clear description of a reproducible, clean initial condition that yields the trends of Kerr (1993) [3]. Ideally, we want an initial condition whose vorticity is purely positive in the upper half of the symmetry plane, which following Kelvin's theorem will remain positive for all subsequent times. These steps were used [3] to massage the vortex profile in order to achieve this:

- 1) The first step in creating the initial profile of the vorticity core is to use an explicit function where the value and all derivatives went smoothly to zero at a given radius. See references in [3] for earlier work that had used a similar profile. To this, a localized perturbation in its position in x was given [9].
- 2) The second step is to remove high-wavenumber noise by applying a symmetric high-wavenumber filter of the form: $\exp(-a(k_x^2 + k_y^2 + k_z^2)^2)$. Kerr (1992) [10] showed the undesirable side-effects if this is not done. However, it has become apparent that the high-wavenumber filter is not sufficient.

B. Effect of a negative region

The upper frames in Fig. 1 come from a reproduction of the squared-off profile of Hou and Li (2006) [8] which follows the procedure above with the exception of using a different high-wavenumber filter. Note the negative region in the lee of the primary vortex and how

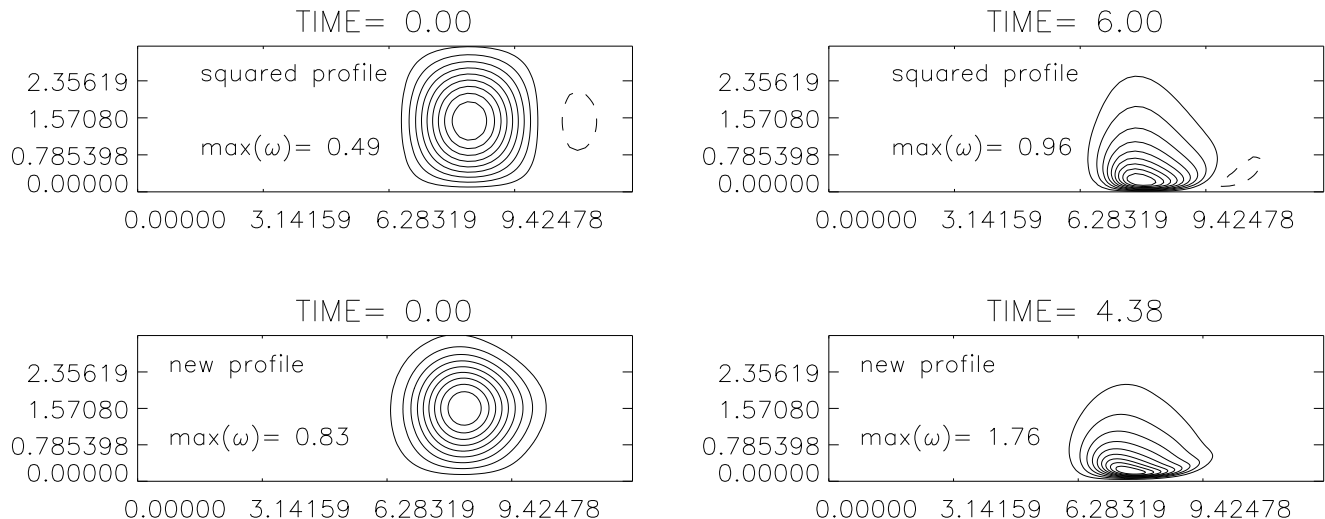


FIG. 1: ω_y in the symmetry plane from two initial conditions for $t = 0$ and for early times with roughly the same growth in $\max(\omega_y)$ in the symmetry plane. The first squared profile is nearly the same as used by Hou and Li (2006) [8] using step 1) with $\max(\omega_y) = 0.49$ in the symmetry plane (over all space $\|\omega\|_\infty = \max(|\omega|) = .67$) and for step 2) a squared-off high-wavenumber filter ($\exp(-a(k_x^4 + k_y^4 + k_z^4))$). Note the large negative vorticity in the lee (right) of the primary vortex as in Hou and Li (2006) [8] (Fig. 2) and how this is entrained underneath the primary vortex at $t = 6$, whereupon the hyperviscous filter will dissipate it. In the new profile step 3 is included: adding positive $\omega_y(z)$. In this case $\max(\omega_y) = 0.83$ in the symmetry plane and over all space $\|\omega\|_\infty = 1.05$. There is no anomalous negative vorticity and numerical solutions require less resolution.

this is sucked underneath the primary vortex at $t = 6$. The $t = 6$ frame represents the vortices simulated with the 36th-order hyperviscosity [8, 11]. For $t > 6$ this secondary vortex is dissipated by the hyperviscosity and circulation is dissipated, meaning these calculations are not faithfully representing the Euler equations. Without the hyperviscosity, numerical noise would dominate as an extra boundary layer needs to be resolved.

C. Final step 3) for purely positive

What is apparently missing from the previous description [3] is the addition of a mean shear designed to remove the final negative regions in the symmetry plane. This was achieved before [3] as part of an interpolation procedure from a uniform mesh to a Chebyshev mesh. Here it is imposed. Details will appear in a full paper. Initial vorticity in the symmetry plane and a slightly later time ($t = 4.38$) are shown. This is the initial condition for which we have now done up to $1024 \times 256 \times 2048$ calculations to assess the scaling proposed earlier [3].

V. A NEW APPROACH FOR DETERMINING WHETHER THERE IS SINGULAR BEHAVIOR OF THE PRIMARY PROPERTIES AND THE ASSOCIATED SCALING.

Once reliable data (according to the criteria discussed above) has been obtained, it is common to interpret it

in terms of power laws and other simple formulae. For example, assume that

$$f(t) \sim C/(T_c - t)^\gamma. \quad (4)$$

To properly find all three free parameters (C , T_c and γ) to a set of points requires a minimization procedure.

Kerr (1993) avoided this by assuming particularly simple values for γ for several quantities. In particular $\gamma = 1$ was assumed for $\|\omega\|_\infty$, for the maximum of the stretching of the vorticity (2) in the symmetry plane: $\max(\alpha)|_{y=0}$, and for the enstrophy production (3). This procedure was extended to the velocity by assuming that $\gamma_u = 1/2$ for $\sup(|u|)$ [5].

While fits with these assumptions gave consistent results for the singular time T_c , this consistency existed only at late times when resolution was becoming questionable. Analysis of this data by two new methods has shown that the lack of scaling at earlier times is due in part to some of the more restrictive assumptions that were made.

A. Three-parameter fitting

Our first indication that earlier assumptions [3, 5] might be incorrect was obtained by allowing γ to be free. The three parameters (C , T_c and γ) were then obtained as follows: by minimizing the sum of squares of the differences between the logarithm of the data and the logarithm of the fit function, with respect to C and γ , allows

one to solve for these two parameters in terms of T_c . Then the sum of squares is further minimized with respect to T_c to obtain all three parameters.

This analysis was applied to $\|\boldsymbol{\omega}\|_\infty$ and Ω_p , the enstrophy production, both of which previously were assumed to have $1/(T_c - t)$ behavior.

It was immediately observed that

- The fitting parameters depended upon the range of times chosen.
- γ in each case was consistently greater than 1.

This would not be inconsistent with known bounds. Recall if power law behavior is expected for $\|\boldsymbol{\omega}\|_\infty$, (1) only requires that $\gamma \geq 1$.

B. Logarithmic time derivatives of enstrophy and $\|\boldsymbol{\omega}\|_\infty$: instantaneous two-parameter fitting

The original analysis would be possible if there is a secondary quantity which must go as $1/(T_c - t)$ if the primary quantity obeys the power law $1/(T_c - t)^\gamma$. An example of a secondary quantity of that sort is the logarithmic time derivative of the primary quantity, which can be computed if we know independently the quantity $f(t)$ and its time derivative $\dot{f}(t)$.

Therefore we propose a new approach to inferring a singular time and identifying the scaling behaviour:

- Find a quantity $f(t)$ whose growth and the growth of its time-derivative can be determined directly. Consider the new function:

$$g(t) = \left(\frac{d}{dt} \log f(t) \right)^{-1} = \frac{f}{\dot{f}} = \frac{1}{\gamma} (T_c - t). \quad (5)$$

Note that the parameter C drops out and the function is linear, so we can predict instantaneous values of γ and T_c by fitting this new function using adjacent points in time.

- Calculating in this manner, using nearest neighbours in time, yields instantaneous predicted singular times $T_c(t)$ and power laws $\gamma(t)$. These instantaneous parameters will generically depend on time.
- See if these converge or relax (as time increases).

Pairs of quantities to which this procedure can be applied are:

- $\|\boldsymbol{\omega}\|_\infty$ and its logarithmic time derivative α_∞ (local stretching at the point \boldsymbol{x}_∞).
- Enstrophy Ω and its production Ω_p (3) where we assume that

$$\Omega \sim \frac{C_\Omega}{(T_c - t)^{\gamma_\Omega}}. \quad (6)$$

- Helicity in the simulated quadrant of space and its production.

This approach is applied to enstrophy and its production on our highest resolution simulations. Because enstrophy and its production are global quantities they converge numerically longer (to $t = 11.25$) than $\|\boldsymbol{\omega}\|_\infty$, for which \boldsymbol{x}_∞ is less than 6 mesh points from the dividing plane for $t > 10$. Running estimates for T_c and γ_Ω are shown in Fig. 2. For the new data (upper frames), the latest data point gives an estimate $T_c \approx 13.16$ and $\gamma_\Omega \approx 0.47$. The bottom frames show the same analysis applied to the data used by Kerr (1993) [3]. Nearly identical power laws are obtained ($\gamma_\Omega \approx 0.50$), with a predicted singular time $T_c \approx 19.69$, greater than in Kerr (1993).

One advantage of finding running estimates of T_c is that it can be used to identify cases that are not singular, or would take an unusually long time to become singular. This is done by looking at the instantaneous estimated value of T_c . If T_c continues to increase with time, then there is evidence for regularity. In both the new calculations and for the data from Kerr (1993), eventually the estimated T_c decreases and relaxes to a finite value. It is quite possible that there is a large pre-factor in front of the power law, which the time dependence of the estimated γ_Ω and C_Ω might be able to shed light on.

This approach assumes smooth values for both quantities in a pair. Unfortunately, we have found that because $\|\boldsymbol{\omega}\|_\infty$ sits on a steep gradient of α , values of α_∞ on the lower resolution mesh were not smooth enough in time to perform this analysis. The analysis will be attempted on the higher resolution ($\|\boldsymbol{\omega}\|_\infty, \alpha_\infty$) data when that additional analysis of the new data sets is available.

C. Convergence studies: Is the evidence for singularity conclusive?

Further tests at higher resolution are needed to support the singular trends seen here. Both current cases (old and new data) could be reliably integrated up to times $t \approx T_c - 2.75$. This would only be the beginning of the asymptotic regime of the potentially singular solution, as is suggested by the late-time behavior of the curves for the predicted singular time T_c in Fig. 2. New calculations in progress should go beyond that barrier and help test the validity of the hypothesis of finite-time singularity.

In this subsection we show resolution studies with n_z fixed to give a flavor of what will be shown in the next paper (we have also made resolution checks with fixed n_x or n_y and varying the other two, not shown here). The resolution study is a classical tool to validate and find reliability times for the numerical results. Another now widely accepted study that we present is a spectral convergence test (Sulem et al., 1983 [12]) used recently by Cichowlas and Brachet (2004) (see [13] and references therein), where the exponential decay of the energy spectrum as a function of the wavenumber is employed to give

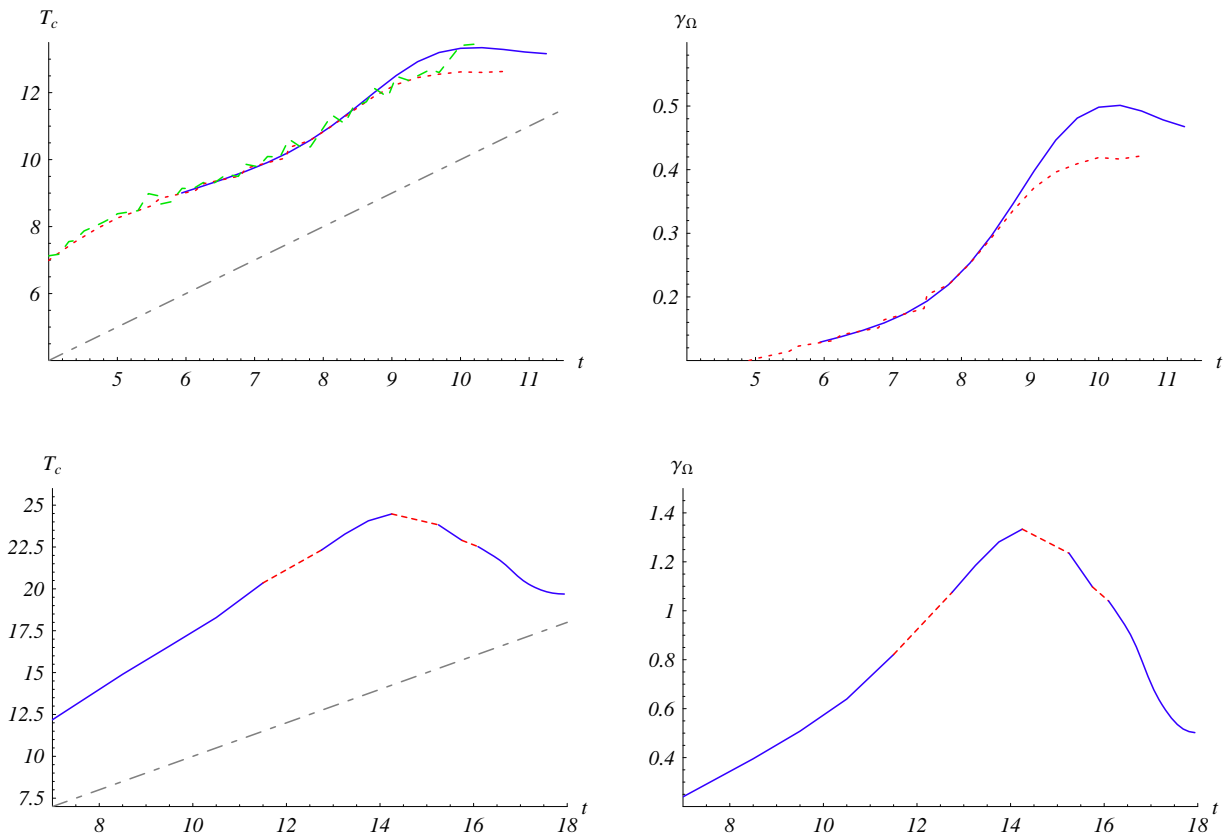


FIG. 2: Upper frames: Resolution study of the predicted singular time T_c and the predicted exponent γ_Ω in the power-law behavior of the total enstrophy Ω using the new data at resolutions: $512 \times 64 \times 2048$ (dashed), $512 \times 128 \times 2048$ (dotted) and $1024 \times 256 \times 2048$ (solid).

Lower frames: Predicted T_c and γ_Ω for the Kerr (1993) data at the highest resolution (solid). Dashed lines denote gaps in data. In the graphs for the predicted T_c , the dash-dotted diagonal lines denote the $T_c = t$ singularity asymptote.

a criteria for the reliability time. Finally we complement the above classical tests with our newly proposed tests of reliability: conservation of circulation through the symmetry plane and conservation of circulation through the dividing plane.

We consider first the behavior of local quantities, in the sense of Section III. Figure 3 (top) is a resolution study of the time dependence of the maximum vorticity; the bottom figure is a $t = 10$ anisotropic energy spectrum $E(k_x, t)$, defined by averaging the Fourier transform $\hat{\mathbf{u}}(\mathbf{k}', \mathbf{t})$ of the velocity field on flat duplicated sheets of width $\Delta k_x = 1$,

$$E(k_x, t) = \frac{1}{2} \sum_{k_x - \Delta k_x/2 < |k'_x| < k_x + \Delta k_x/2} |\hat{\mathbf{u}}(\mathbf{k}', \mathbf{t})|^2.$$

Following [13], we fit: $\log E(k_x) = C - n \log(k_x) - 2\delta k_x$ (solid line in the figure). The test consists in monitoring the parameter δ as a function of time. The idea is that δ , being the width in the complex plane of the analyticity strip of the velocity field, should always be numerically resolved, at least by the mesh size. Another way

to look at this condition is to ask that the contribution of the exponential term to the change of $\log E(k_x)$ from the largest to the smallest scale allowed by the numerical resolution, be greater than a prescribed factor. In more explicit terms, we can only fully trust the simulation up until the condition $\delta k_x^{\max} \geq 1$ is violated, where $k_x^{\max} = n_x/3$ is the maximum relevant wavenumber of the Fourier representation. Notice that different authors use different factors in the RHS of the last inequality. For our $t = 10$ spectrum in resolution $1024 \times 256 \times 2048$ we obtain $\delta k_x^{\max} \approx 1.07$, and therefore our simulation is validated by this method up to $t = 10$. In this way we could extrapolate the convergence of $\|\boldsymbol{\omega}\|_\infty$ up to $t = 10$, whereas a conservative extrapolation based solely on the resolution study in figure 3 (top) would see the $1024 \times 256 \times 2048$ computation converged up to $t = 9$.

We consider now the behavior of 2D integral quantities. Due to its 2D character, enstrophy in the symmetry plane $\Omega_{SP} = \int_{y=0} \omega_y^2 dx dz$, shown in figure 4 (top), is a more sensitive measure than total enstrophy Ω (eq.(3), figure not shown), which converges more rapidly than Ω_{SP} . A

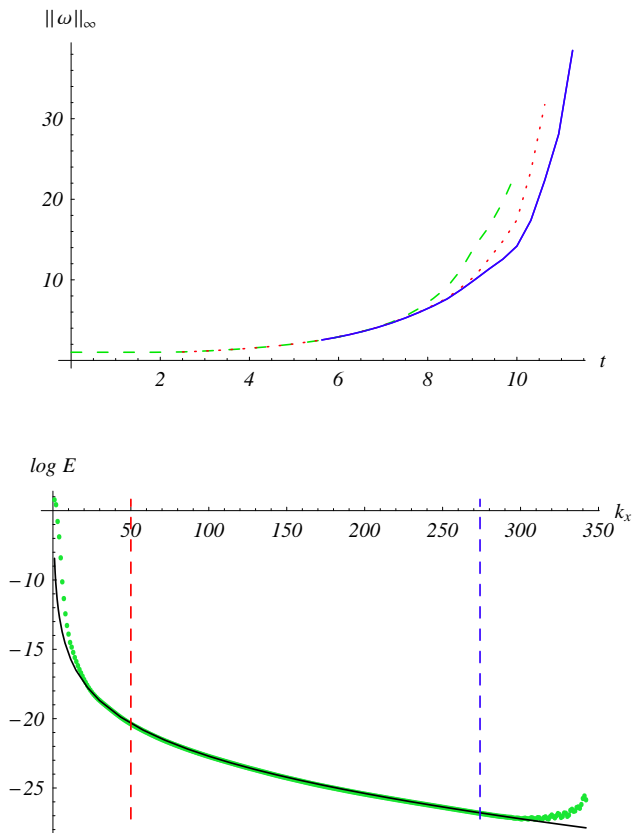


FIG. 3: Top: Resolution study of $\|\omega\|_\infty$, for resolutions $n_x \times n_y \times n_z$ of: $512 \times 64 \times 2048$ (dashed), $512 \times 128 \times 2048$ (dotted) and $1024 \times 256 \times 2048$ (solid). Bottom: Anisotropic energy spectrum (direction k_x) at time $t = 10$ for resolution $1024 \times 256 \times 2048$. Points correspond to numerical data. The solid curve corresponds to the fit of the spectrum according to $\log E(k_x) = C - n \log(k_x) - 2\delta k_x$, where the fit interval is defined by the vertical dashed lines.

conservative extrapolation would imply convergence of Ω_{SP} up to times $t \lesssim 11$.

Figure 4 (bottom) is a resolution study of the normalized error in the conservation of circulation through the dividing plane σ_z . We observe that, for a given resolution, the numerically induced deviation in σ_z becomes unstable after a certain time. Errors (and fluctuations thereof) less than 10^{-4} are acceptable, as long as they are stable. Then, a reasonable reliability time can be defined for each resolution as the time when the error in σ_z attains its last extremum before the instability takes over. According to this criteria we conclude that the simulation at resolution $512 \times 128 \times 2048$ (dotted line) is converged up to $t \approx 10.7$ and the simulation at resolution $1024 \times 256 \times 2048$ (solid line) converges up to $t \approx 11.25$. In order to display the unstable behavior of the mid-resolution simulation (dotted line), we show data beyond its reliability time.

Finally we return to Fig. 2, considering all three reso-

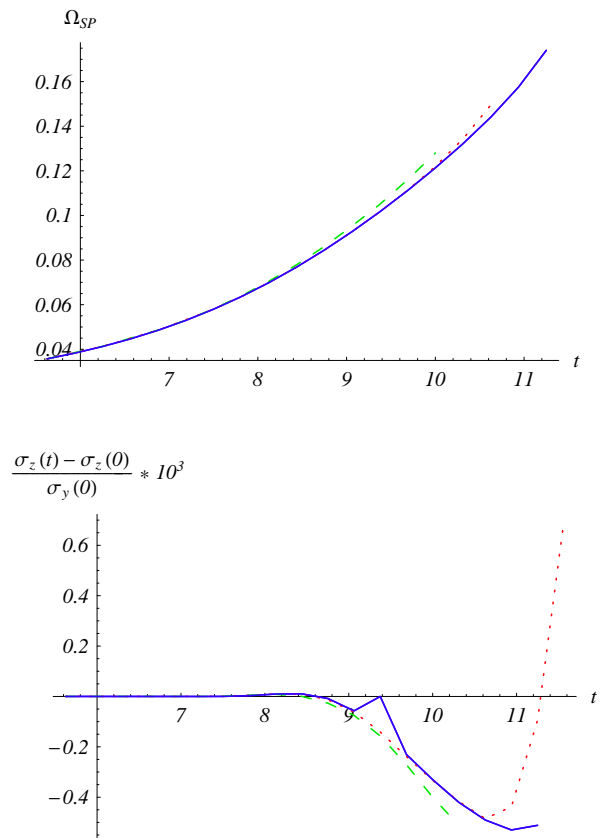


FIG. 4: Resolution study of: the enstrophy in the symmetry plane Ω_{SP} (top); the error in the circulation through the dividing plane σ_z normalized with the initial circulation through the symmetry plane σ_y (bottom), for resolutions $512 \times 64 \times 2048$ (dashed), $512 \times 128 \times 2048$ (dotted) and $1024 \times 256 \times 2048$ (solid).

lutions. For each resolution, T_c has a peak for $t \approx 9-10$, and then asymptotes, well within the reliability time for the highest resolution. Similar trends towards convergence appear for γ_Ω . The key question regarding the existence of a finite-time singularity is if the curve for predicted T_c crosses the asymptote $T_c = t$ (dashed-dotted line) in a finite time or not, but we need further tests at higher resolutions (to be shown in a future paper) in order to conclude on these matters.

We have enough resolution to conclude that the power laws are not the ones proposed in Kerr (1993,2005) [3, 5] but not enough resolution to reach definitive conclusions on the singular behavior, since $\|\omega\|_\infty$ does not converge as rapidly as the volumetric quantities studied.

VI. GRAPHICS

In this section, 3D isosurface contours of the vorticity modulus are shown, corresponding to the simulation of

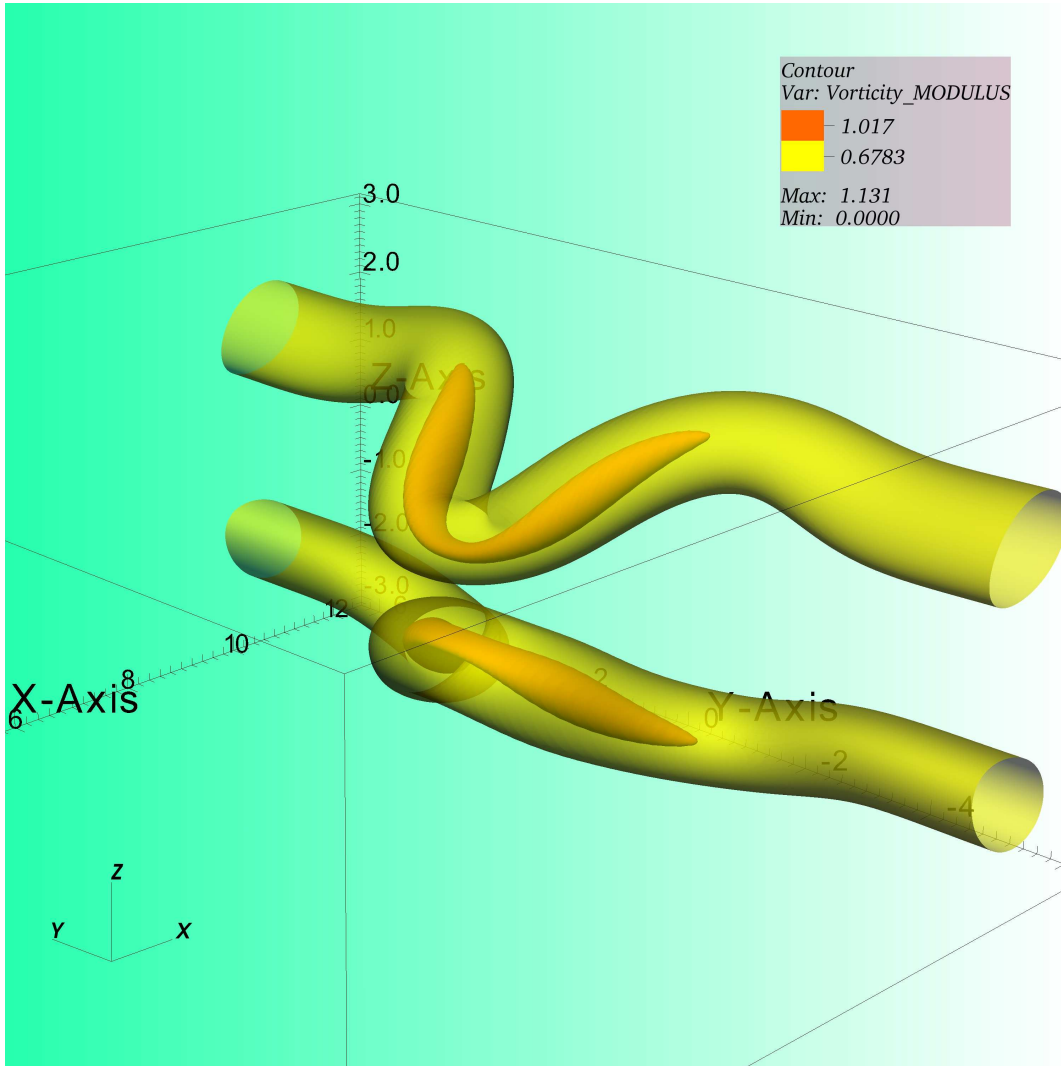


FIG. 5: Euler anti-parallel vortices in full periodic domain near $t = 2.51$. Bright (yellow online) tubes are isosurface contours of vorticity modulus corresponding to 60% of the instantaneous maximum of vorticity modulus. Dark (red online) elongated blobs are isosurfaces corresponding to 90% of the maximum of vorticity modulus.

initially anti-parallel vortices, using a resolution of $512 \times 128 \times 2048$ in the fundamental quarter of the full domain, corresponding to an effective resolution of $512 \times 256 \times 4096$ in the full domain. For memory-optimizing purposes, the output data used to make the figures has an effective resolution of $512 \times 128 \times 1024$, corresponding to a memory size of 65 MB. The freeware visualization program VisIt has been used to make the plots.

Fig. 5 shows the vortices after some time of evolution in the whole periodic domain. The large tubes are isosurfaces corresponding to 60% of the maximum vorticity modulus. These tubes cross along the periodic Y-Axis and deform notably near the symmetry plane ($y = 0$). The elongated blobs in the interior of the tubes are iso-

surfaces corresponding to 90% of the maximum vorticity. These isosurfaces are very localized and flattened near the symmetry plane.

Fig. 6 shows successive snapshots at later stages of the flow, of isosurfaces corresponding to the following percentages of the instantaneous value of the maximum vorticity modulus: from outer to inner contours, 40%, 60%, 80% and 90%. Only half of the total domain is shown so that a section of the isosurfaces through the symmetry plane ($y = 0$) is visible. The snapshots are all seen from the same angle and with the same zoom with respect to the fixed box. To read the snapshots going forward in time one advances from left to right and from top to bottom.

The flattening in the z -direction results in structures similar to flattened pillows with some curvature in x (and less in y) that becomes more pronounced at the later times along the cut at the symmetry plane. These empirical observations provide further support for the choice of anisotropic resolution in the simulations.

VII. LOOKING FORWARD

The calculation reported here was the largest possible on the Warwick SGI Altix with our code. In the near future we will have a cluster capable of simulating a $2048 \times 1024 \times 4096$ mesh. We might also use UK national computing resources.

Once our new cluster arrives we anticipate the following calculations:

- Further tests to determine if an initial condition closer to that of Kerr (1993) [3] can be obtained.
- After further resolution checks, at least one calculation on a $2048 \times 512 \times 4096$ mesh either on the new profile here or that of Kerr (1993) [3].
- At least one modest resolution calculation on the square-off initial condition of Fig. 1.
- Our goal in high resolution calculations will be to include spectral convergence tests, in particular the analyticity strip method (Sulem et al. [12], see also [13, 14] and references therein) which gives independent evidence of singular/nonsingular behavior of the flow and allows one to extrapolate the convergence of $\|\omega\|_\infty$.
- Convergence of $\|\omega\|_\infty$ and other local quantities should allow us to study regularity bounds from

Constantin, Fefferman and Majda [4] and from Deng, Hou and Yu [15].

The finite-time singularity hypothesis of the three-dimensional, incompressible Euler equations, leads to conclusions that are in qualitative agreement with Kerr (1993) [3]. However, we have found that the previously proposed scaling laws and estimated singular time must be modified.

One possible outcome which will require further investigation is whether constant circulation is trapped within the collapsing region. If this is confirmed, the two length scaling parameterization proposed [5] cannot be correct.

It is anticipated that in addition to these much higher resolution anti-parallel calculations, there will soon be new high-resolution calculations of the Kida-Pelz flow (anticipated in these proceedings by the contribution of Grafke et al. [16]) and the Taylor-Green calculations initiated by Brachet et al. (1983) [17] will soon be continued by Brachet. If these prove to be singular, and anti-parallel, it is possible that they will reproduce the scalings hinted at here.

Acknowledgments

We acknowledge discussions with C. Bardos, J. D. Gibbon, R. Grauer, T. Hou, S. Kida, R. Morf, K. Ohkitani, E. Titi and other participants in Euler250. We thank U. Frisch and co-workers for organizing this excellent symposium. Support for this work was provided by the Leverhulme Foundation grant F/00 215/AC. Computational support was provided by the Warwick Centre for Scientific Computing.

-
- [1] L. Euler, *Principia motus fluidorum*. *Novi Commentarii Acad. Sci. Petropolitanae* 6 (1761) 271–311.
- [2] J. T. Beale, T. Kato and A. Majda, Remarks on the breakdown of smooth solutions for the 3D Euler equations. *Commun. Math. Phys.* 94 (1984) 61.
- [3] R.M. Kerr, Evidence for a singularity of the three-dimensional, incompressible Euler equations. *Phys. Fluids* 5 (1993) 1725–1746.
- [4] P. Constantin, C. Fefferman and A. Majda, Geometric constraints on potentially singular solutions for the 3D Euler equations. *Comm. Partial. Diff. Eqns.* 21 (1996) 559–571.
- [5] R.M. Kerr, Velocity and scaling of collapsing Euler vortices. *Phys. Fluids* 17 (2005) 075103.
- [6] R. Grauer, C. Marliani and K. Germaschewski, Adaptive mesh refinement of singular solutions of the incompressible Euler equations. *Phys. Rev. Lett.* 80 (1998) 41774180.
- [7] P. Orlandi and G. Carnevale, Nonlinear amplification of vorticity in inviscid interaction of orthogonal Lamb dipoles. *Phys. Fluids* 19 (2007) 057106.
- [8] T.Y. Hou and R. Li, Dynamic depletion of vortex stretching and non-blowup of the 3-D incompressible Euler equations. *J. Nonlin. Sci.* 16 (2006) 639–664.
- [9] R.M. Kerr and F. Hussain, Simulation of vortex reconnection. *Physica D* 37 (1989) 474–484.
- [10] R.M. Kerr, Evidence for a singularity of the three-dimensional incompressible Euler equations. in: *Topological aspects of the dynamics of fluids and plasmas* (Eds.), G.M. Zaslavsky, M. Tabor and P. Comte, Proceedings of the NATO-ARW workshop at the Institute for Theoretical Physics, University of California at Santa Barbara. Kluwer Academic Publishers, Dordrecht, Netherlands., 1992, pp. 309–336.
- [11] T.Y. Hou and R. Li, Computing nearly singular solutions using pseudo-spectral methods. *J. Comp. Phys.* 226 (2007) 379–397.
- [12] C. Sulem, P.-L. Sulem and H. Frisch, Tracing complex

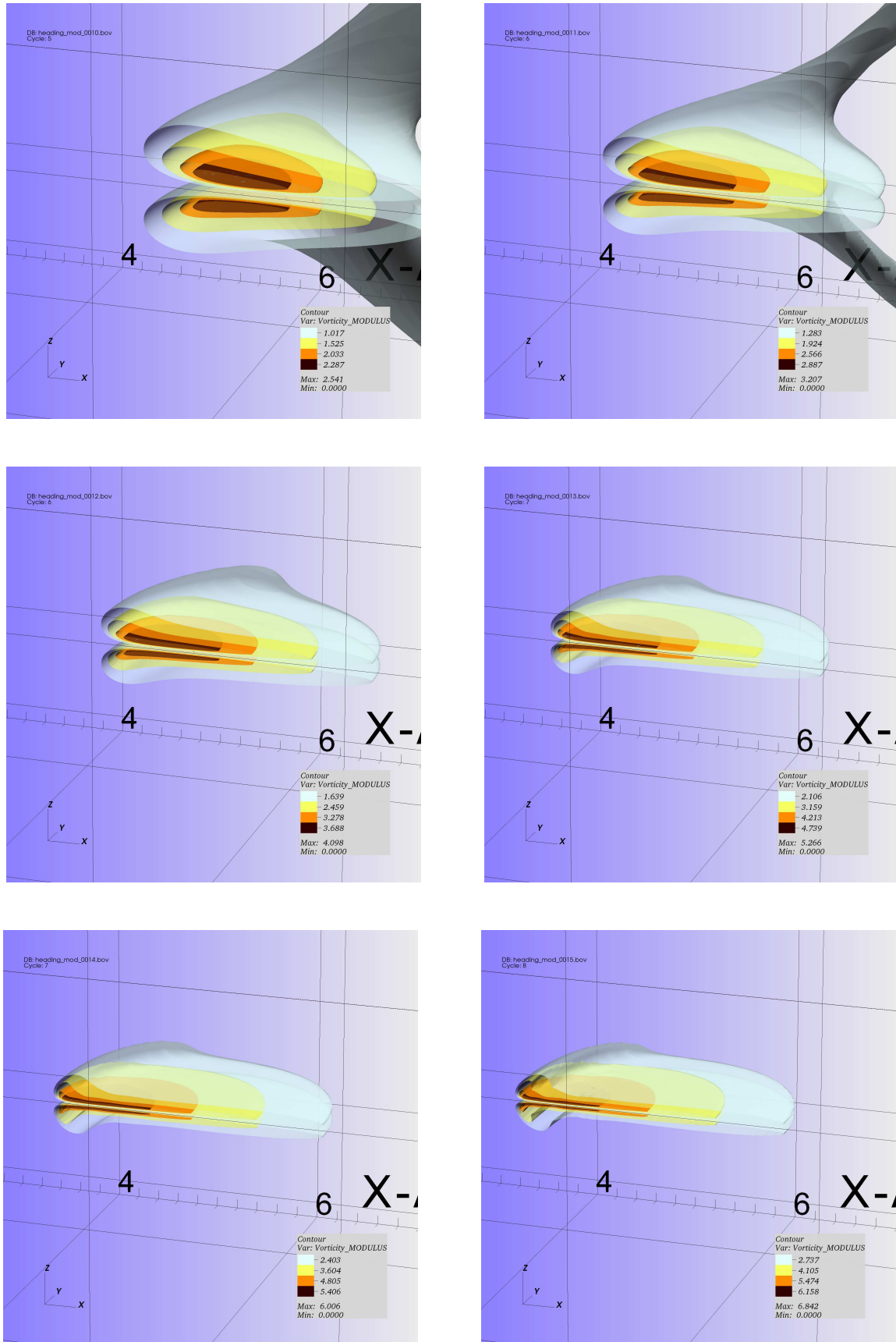


FIG. 6: From left to right, and from top to bottom: six successive, zoomed snapshots of the Euler anti-parallel vortices at times $t = 5.625, 6.25, 6.875, 7.5, 7.8125, 8.125$. The contours are sectioned through the $y = 0$ symmetry plane, to facilitate the view of the structures. The contours are isosurfaces of vorticity modulus corresponding, respectively from outer to inner, to the 40%, 60%, 80% and 90% of the value of the instantaneous maximum vorticity modulus.

- singularities with spectral methods. *J. Comp. Phys.* 50 (1983) 138-161.
- [13] C. Cichowlas and M.E. Brachet, Evolution of Complex Singularities in Kida-Pelz and Taylor-Green Inviscid Flows. *Fluid Dynamics Research* 36 (2004) 239-248.
- [14] U. Frisch, T. Matsumoto and J. Bec, Singularities of Euler flow? Not out of the blue! *J. Stat. Phys.* 113 (2003) 761-781.
- [15] J. Deng, T.Y. Hou and X. Yu, Improved geometric condition for non-blowup of the 3D incompressible Euler equation. *Commun. Partial Diff. Equns.* 31 (2006) 293-306.
- [16] T. Grafke, H. Homann, J. Dreher, R. Grauer, Numerical simulations of possible finite time singularities in the incompressible Euler equations: comparison of numerical methods (2007), these Proceedings.
- [17] M.E. Brachet, D.I. Meiron, S. A. Orszag, B. G. Nickel, R.H. Morf and U. Frisch, Small-scale structure of the Taylor-Green vortex. *J. Fluid Mech.* 130 (1983) 411-452.